Chapter 5

Spectro-microscopic imaging of organic layers

In this work, UV-PhotoElectron Emission Microscopy (UV-PEEM) and LEEM have been proven to be very useful for investigation of dynamical properties of organic layer growth. Furthermore, laterally resolved NEXAFS has contributed to the understanding of the bond properties at the interface and the molecular orientation everywhere in the film.

In figure 5.1 three images of the same sample region show exemplarily how strongly these three methods differ. A quick comparison between images (a) and (b) shows contrast inversion, while in figure (c) the 3d-islands, marked by the corners of the red triangle, appear as a smaller bright region with a darker ring around it. Furthermore, white lines in image (a) appear dark in (c).

This chapter is dedicated to the understanding of these imaging properties and the identification of the various regions and defects. The three methods have the low kinetic energy of the electrons (below 20 eV) in common. In the first part of the chapter we investigate two metal surfaces, Ag(1 1 1) and Au(1 1 1), and show that the photo-emission process with a Hg-short arc lamp is very sensitive to the work function of the substrate, and to the film thickness. Moreover we show that the electron Inelastic Mean Free Path (IMFP) in an organic film is much shorter than what is expected from the inspection of the so-called *universal IMFP curve*.

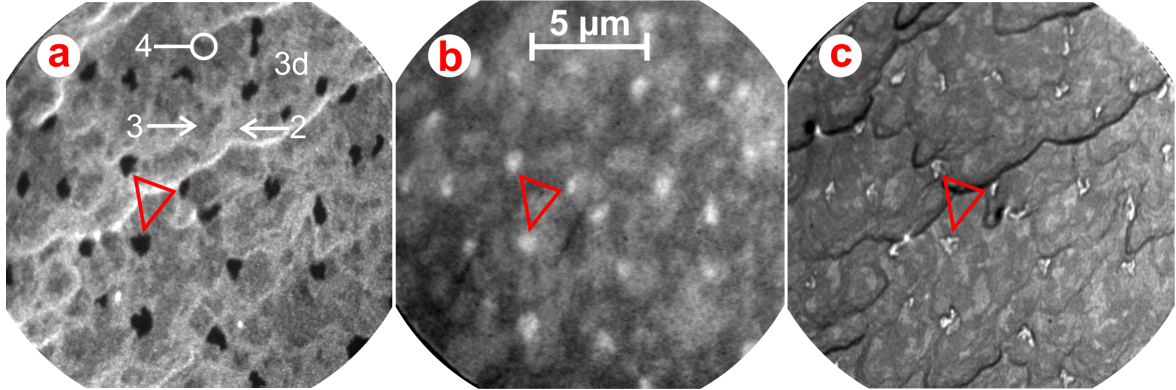Following this UV-PEEM section, we focus on the laterally resolved NEXAFS and

Figure 5.1: Three images of the same region of the sample using three different techniques: (a) UV-PEEM, (b) NEXAFS-PEEM, (c) LEEM. In image (a) the thicknesses of the layers, from 2 to 4 and 3d-islands, are indicated. In each image the corners of a red triangle identify identical 3d-islands used as a reference. The scaling bar of 5 μm in figure (b) applies to all images.

evaluate the same quantities to find that the IMFP obtained from the secondary electrons is slightly higher. In the last part of the chapter we discuss the structural information that can be studied with LEEM, e.g. domains with different orientation. We will also inspect the quantum interference in the thin film and propose future measurements for a better basic understanding of these organic molecular crystals.

5.1 Image contrast in UV-PEEM of organic layers on metals

PEEM is not only sensitive to work function changes, but also a high sensitivity on the deposited thickness is achieved. With a mercury short arc lamp (Hg-lamp) photons of maximum energy of 4.9 eV are used for the photoexcitation process. This *low* photon energy (as compared to x-ray radiation) is in the typical range of work functions of metals from 4 to 5.5 eV. Therefore the UV-PEEM method is sensitive to work function changes. The two images in figure 5.2.a and 5.2.c show how significantly the imaging of the Ag(1 1 1) and the Au(1 1 1) surfaces differ in brightness. The two images are significantly different (in brightness) and a large difference in work function is to be
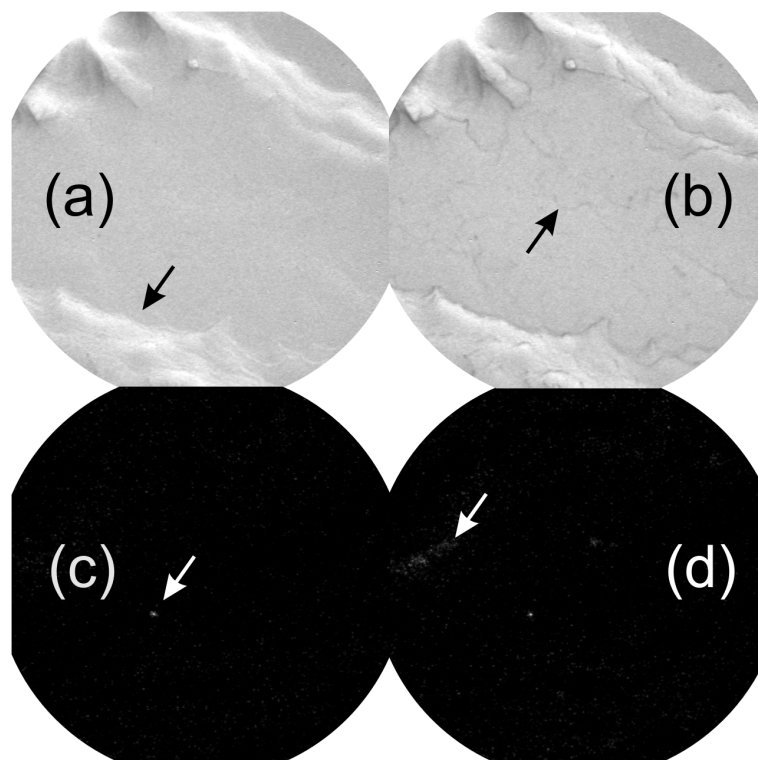
Figure 5.2: UV-PEEM images of the (a) clean and (b) PTCDA step-decorated Ag(1 1 1) surface at 375 K, and of the (c) clean Au(1 1 1) surface at 423 K, and (d) the start of PTCDA nucleation. The arrows in the images point out: (a) step bunches, (b) single steps, (c) a surface defect, (d) first layer nucleation of PTCDA. The field of view in all four images is 25 μm. Notice that images (c) and (d) *are* meant to appear dark in the printed version.

expected. This is in agreement with the work functions reported in table 3.2 on page 26. Owing to these strong differences in work function, between Ag(1 1 1) and Au(1 1 1), the discussion of the contrast mechanism will be addressed in two dedicated sub-sections.

5.1.1 The Ag(1 1 1) substrate

In order to simplify the understanding of the contrast formation during heterogeneous growth it is useful to first discuss the two limits of the growth, i.e. the clean Ag(1 1 1) surface and the (1 0 2) surface of crystalline PTCDA on Ag(1 1 1). Then the intermediate situation of one to a few layers of PTCDA on the Ag(1 1 1) surface will be examined. The justification for such an approach stems from the assumption that a thick enough layer will exhibit the properties of the bulk material. According to earlier spectroscopic work [47], the bulk properties, with respect to the energy levels of the highest occupied molecular orbital (HOMO) and lowest unoccupied molecular orbital (LUMO), are already exhibited for a thickness greater that *one single PTCDA layer*. This might be an oversimplification because thermal desorption [38] and our own PTCDA growth experiments (described in chapter 7) have shown that the first *two* deposited layers have different desorption temperatures and growth properties with respect to the higher layers. However, different energy levels in the bilayer, with respect to the thicker — *bulk like* — PTCDA, have so far not been spectroscopically measured and thus are presumably too small for detection. For this reason, in the following we will restrict the discussion of the intermediate region to the presence of one single layer of PTCDA on a Ag(1 1 1) surface.

The energy level diagram within this model of the clean Ag(1 1 1) surface, a single layer of PTCDA on Ag(1 1 1) and the (1 0 2) surface of crystalline PTCDA on Ag(1 1 1), was shown in figure 3.3 on page 28, as adapted from [47]. In the two extreme regions, of the clean Ag(1 1 1) surface and the (1 0 2) surface of crystalline PTCDA on Ag(1 1 1), photoemission using a laboratory Hg-short-arc lamp is determined by the classical three step model [1]:

i) Photoexcitation of an electron in the solid (Fermi's Golden Rule),

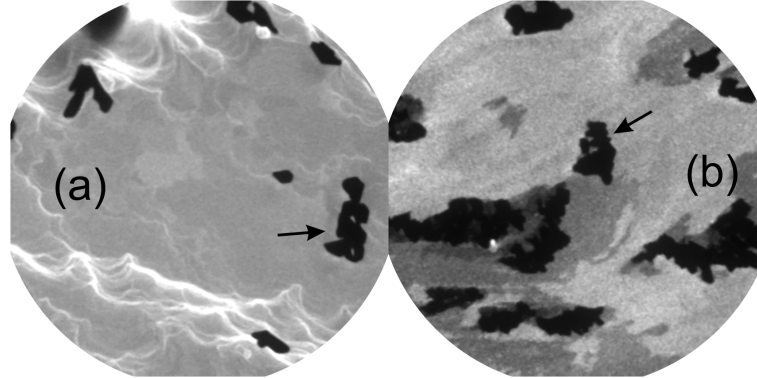ii) Propagation of the photoexcited electron to the surface (attenuation of the electron wave).

Figure 5.3: UV-PEEM images of 5 nominal layer of PTCDA deposited on the (a) Ag(1 1 1) and (b) Au(1 1 1) surfaces. The arrows indicate 3D islands with an estimated thickness of 100 to 200 nominal layers. The field of view in all four images is 25 μm. And the substrate temperatures are 375 K and 423 K for Ag and Au, respectively.

iii) Escape of the electron from the solid into the vacuum (work function).

The obtained photoemission intensity, for the clean Ag(1 1 1) surface, is high (signal-to-noise ratio), and images such as those shown in figure 5.2.a and 5.2.b are obtained. The kinetic energy of the photoemitted electrons is lower than 0.1 eV. The photoemission process takes place in a quite small volume, of a few nanometers (if the emitting atom is in the bulk) or even only in an atom (if this is at the surface). This property of a local probe is used in PEEM, and it allows for the identification of defects on the Ag(1 1 1) surface like step bunches (indicated by the arrow in image 5.2). Upon step decoration, e.g. with PTCDA, also single steps can become visible as indicated by the arrow in image 5.2.b.

For the (1 0 2) surface of crystalline PTCDA on Ag(1 1 1), emission from the HOMO can be excluded because the DOS at the Fermi level is zero and the HOMO lies 2.5 eV below it (right side of figure 3.3). Furthermore, two-photon photoemission processes can be neglected under our experimental conditions. For these reasons, the UV-PEEM intensity of 3d-islands, with high thickness above 11 nominal layers, is zero as shown by the arrows in image 5.3.a.

At the PTCDA/Ag(1 1 1) interface new electronic states are formed by hybridization of the molecular and substrate orbitals, as shown in the center of figure 3.3. The experimental observation of the hybridization of the LUMO of PTCDA with the s-states

of Silver is presented in section 8.2 on page 103. The change in photoemission intensity upon deposition of one layer of PTCDA is described by the following arguments:

j) the work function is increased to 4.9 eV, thus reducing the substrate electron emission by cutting off some fraction,

jj) the emission from the substrate is reduced by elastic and inelastic scattering of the emitted substrate electrons migrating through the organic layer (attenuation),

jjj) a new emission channel, right below the Fermi level, is opened which arises from the hybridization (and partial filling) of the LUMO of PTCDA with the s-states of Ag.

The deposition of one layer of PTCDA on Ag(1 1 1) decreases drastically the intensity by a factor of about 7 as shown in figure 5.4.a. For this reason, the work function change j) and the damping effect jj) are dominating the PEEM contrast, whereas the intensity increasing effect of jjj) is apparently small. This is most likely due to a low photoemission cross section in this photon energy range.

After the first layer the intensity decrease is exponential, as shown by the fit in figure 5.4.a. Therefore we conclude that the dominating effect, after the first layer has been deposited, is the damping jj) and no further decrease of the work function is observed in agreement with integral work function measurements by *Kilian* [38].

The attenuation effect jj) can be further analyzed and compared to what is known as the "universal curve" for the Inelastic Mean Free Path (IMFP) λ of electrons in a solid shown in figure 5.5. The IMFP is defined as the distance over which the probability of an electron escaping without significant energy loss due to inelastic processes drops to e^{-1} of its original value [58]. By monitoring the decrease in signal with increasing thickness at normal incidence angle, the quantity measured is known in the literature as the Effective Attenuation Length (EAL). The reason for this is that we observe a decrease in signal also for electrons that have elastically scattered away from normal emission. Thus, we expect that the measured EAL is lower than the real IMFP. We will in any case refer in the following directly to the IMFP, in order to correlate our results the theoretically predicted *ideal* IMFP value. As compared to integral measurement, the microscopic estimation of the IMFP relies on an accurately determined film thickness.
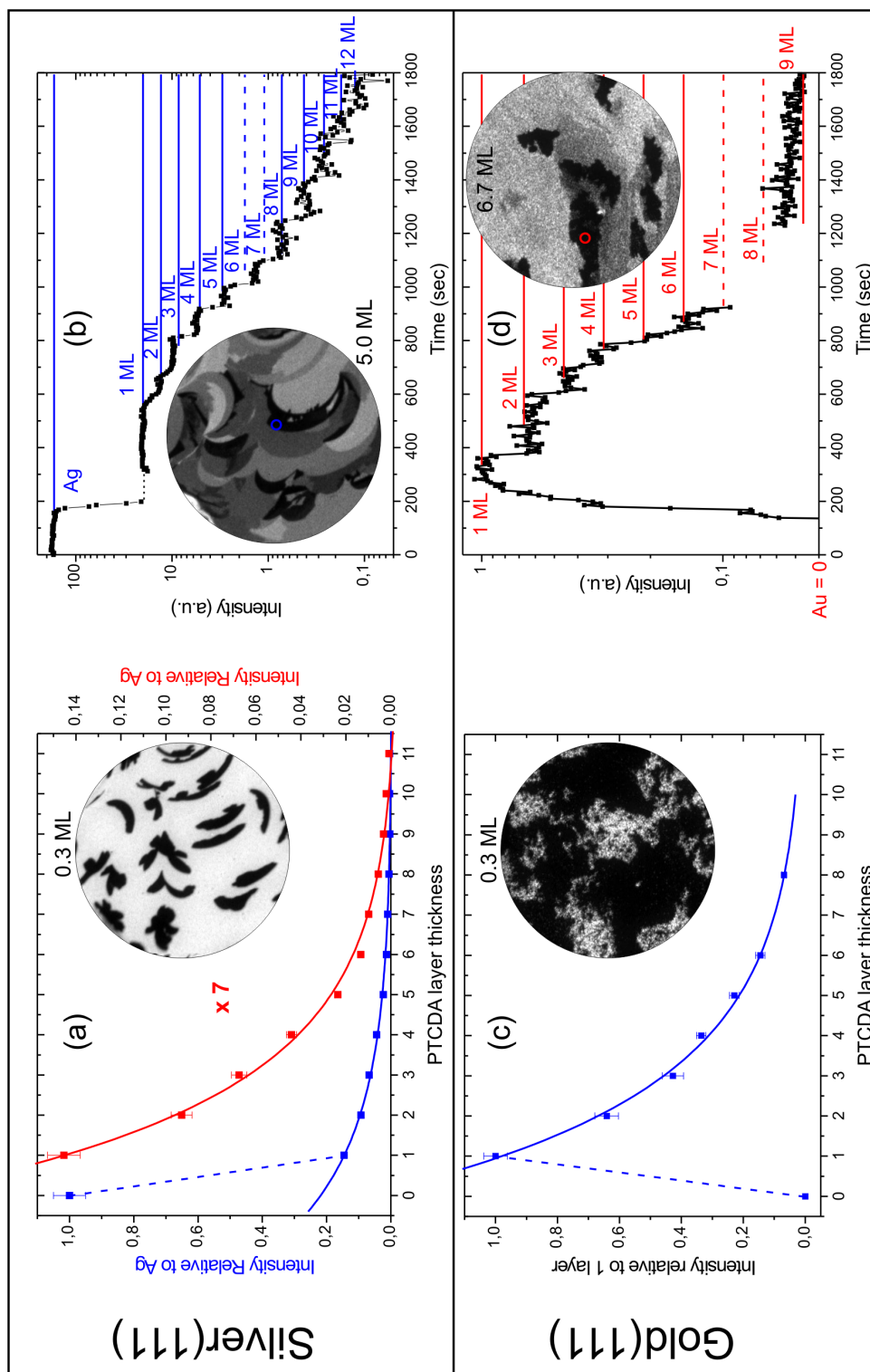
Figure 5.4: Intensity decay in UV-PEEM: photoemission intensity relative to the clean (a) Ag(1 1 1) and (c) Au(1 1 1) substrate vs. PTCDA layer thickness, given in units of nominal PTCDA monolayers. The data have been fitted with an exponential function, see text for details. Intensity of the surface area enclosed in the blue (b) and red (d) circles (inside the images in the inset) during deposition of PTCDA on (b) Ag(1 1 1) and (d) Au(1 1 1).
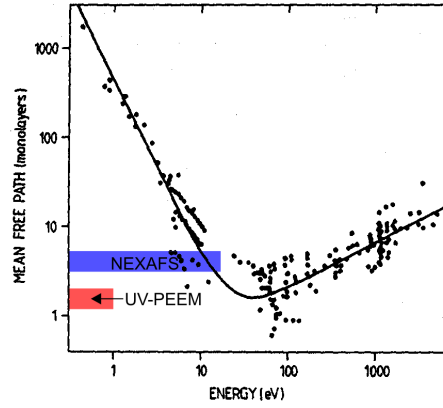
Figure 5.5: "Universal" inelastic mean free path curve. The IMFP of electrons in PTCDA measured by UV-PEEM is marked in red, while NEXAFS is marked in blue. Curve adapted from [58].

An exponential least square fit of the relative intensity, with $n = 2$ to 11 layers, using the function:

$$I(z) = I_0 \exp\left(-\beta n\right) \tag{5.1}$$

gives as a result for β of 0.43 ± 0.02 layers^{-1}. The IMFP given by:

$$\lambda = \frac{1}{\beta} \tag{5.2}$$

yields 2.34 ± 0.08 layers of PTCDA corresponding to 0.76 ± 0.03 nm assuming an interlayer distance of β-PTCDA of 0.325 nm [36].

Although the obtained value of 0.76 nm has been carefully measured, with UV-PEEM experiments using a Hg-short arc lamp, the following can be pointed out. The measured value does not *only* include the normal emission (90°), but a wider acceptance angle around the normal. In a microscope normal incidence can only be obtained if the contrast aperture is reduced to the minimum. This condition however reduces excessively the emission and it has therefore not been adopted. We therefore choose for an aperture selecting an angle of $\sim 30°$ around the surface normal. Another concern

is the fact that the emitted electrons are not monoenergetic but have a kinetic energy in the range between 0 and 1 eV. The energy dependence of the IMFP in this energy region is therefore unknown.

As compared to metals, the IMFP of 0.76 nm is rather short. The energies at which we measured the IMFP are lower than 1 eV. We have therefore marked in red a region in figure 5.5 identifying the IMFP of electrons in a PTCDA film as measured using a Hg-short arc lamp. The reasons for such a discrepancy from the general tendency of the "universal curve", which is after all not so *universal*, can be related to a high cross section for inelastic processes at low kinetic energies. One of the processes that can increase the cross section by several orders of magnitude is the coupling of a vibrational excitation with the formation of a transient anion state (resonance) resulting from the temporary trapping of an electron in unoccupied molecular orbitals [59, 60]. Such processes have been found in HREELS investigations of PTCDA on the different substrate InAs(111) [61]. In this experiment the excitation function shows a substantial enhancement in the vibrational mode intensity below 2.5 eV for a wide range of film thicknesses. This behavior is consistent with vibrational excitations via resonant scattering of the incident electron captured in anti-bonding molecular orbitals, hence a low IMFP can be justified.

5.1.2   The Au(1 1 1) substrate

Due to the ~ 0.5 eV higher work function, there is no photoemission for the Au(1 1 1) surface, as shown in image 5.2.c. Photoemission occurs only from defects or regions where the substrate is not clean. Or sharp objects have been formed resulting in a lower work function or higher local electrical field (which in turn lowers the local work function) as indicated by the arrows in images 5.2.c and 5.2.d.

The plot in figure 5.4.c shows the measured intensity, normalized to the first layer, relative to the thickness of the organic film. Notice that before deposition the intensity is *zero*. After deposition of one layer the work function is decreased by 0.4 eV [38] to 4.9 eV. Again we do not observe any change in the work function after the first layer. Because of an exponential decrease of the intensity (as shown in the plot in figure 5.4) this is related to the attenuation of the electrons, whereas a change in the work

Table 5.1: Inelastic mean free path: Experimental results of IMFP values for the Hg-lamp photoemission from Ag(1 1 1) and Au(1 1 1) surfaces covered with PTCDA.

	Measured IMFP [nm]
Ag(1 1 1)	0.76 ± 0.03
Au(1 1 1)	0.85 ± 0.04

function would result in a non-exponential change of the intensity (as observed for the transition from the clean to the covered substrate).

As compared to the case of Ag(1 1 1), the overall number of identifiable layers is reduced to 8. The reason for this can be that the work function of the thick PTCDA film on the Au(1 1 1) surface is slightly higher than that resulting from the thick PTCDA film on the Ag(1 1 1) surface. Also a small difference in the density of states at the Fermi level could cause such a difference.

An exponential least square fit of the intensity using equation (5.1) and starting from the first layer, is shown in figure 5.4.c. It results in a value of β of 0.38 ± 0.02 layers^{-1}, corresponding to an IMFP of 2.6 ± 0.1 β-PTCDA layers or $\lambda = 0.85 \pm 0.04$ nm. As for the Ag(1 1 1) surface, the same considerations apply to the Au(1 1 1) surface regarding the acceptance angle and the kinetic energy of the electrons.

The results obtained for the two substrates are shown in table 5.1.2. There is a very small difference in the IMFP, of $\Delta = 0.1$ nm, depending on what substrate is used. This difference can be simply attributed to slightly different sample preparation conditions. For example, the presence of sub-surface impurities, or facets or high step densities[1] would significantly alter the work function of the metal, which in turn would alter the range of available kinetic energies of the photoemitted electrons detected. Furthermore structural differences in the thin film properties on the two substrates, such as variations of the density of point defects or dislocations, would influence the scattering of electrons. The intrinsically different bond properties of the molecules at the interface with the two metals can also affect the IMFP due to a different availability of vibrational excitations.

---

[1]The steps are not observable on the Au(1 1 1) surface with UV-PEEM.

5.2 Image contrast in laterally-resolved NEXAFS

A NEXAFS spectrum with a PEEM microscope is acquired by scanning the photon energy and imaging the secondary emission. The basics of photo absorption process and the method are described in [62].

The NEXAFS spectra in the center of figure 5.6 result from an integration of a stack of images in the areas marked in the XPEEM images. The x-ray light was linearly polarized with an electrical field vector almost perpendicular to the surface[2]. In the image on the right side three distinct regions are observable and marked by letters: (a) 3d-island, (b) closed second layer and (c) non-closed third layer. The image contrast depends on the energy. At the beginning of the spectra, i.e. at photon energies lower than $h\nu = 283$ eV (below the first resonance), the signal of the second layer is highest and that of the 3D-islands is lowest (see left image in figure 5.6). This is because the photoelectrons, which are predominantly originating from the underlying silver substrate[3], are attenuated by elastic and inelastic scattering in the thin organic film.

After onset of the x-ray absorption, i.e. where the three lines cross at about 283.7 eV, the highest signal is obtained from the 3D-islands and the lowest from the second layer. In this case, as opposed to the pre-resonance situation, most of the intensity is generated in the film and, up to a saturation thickness, it is thickness dependent.

Chapter 8 is dedicated, among other things, to the discussion of the molecular orientation of PTCDA on the Ag(1 1 1) surface. Here we (correctly) assume the same molecular orientation, with the perylene core parallel to the surface, everywhere on the substrate. The resulting intensity is only dependent on thickness, the energy, and the polarization of the x-rays. For the purpose of the following discussion the influences of the interface to the spectra can be neglected.

From a more general point of view the contributions to the intensity, that determine the contrast in the images, can be separated into following contributions:

1. Throughout the spectra it is assumed that the intensity emitted by the substrate

---

[2]The actual angle is 20° to the surface normal.

[3]The cross-section for the emission from the organic thin film is probably low in this energy region and results in a negligible photoemission if compared to that arising from the substrate.
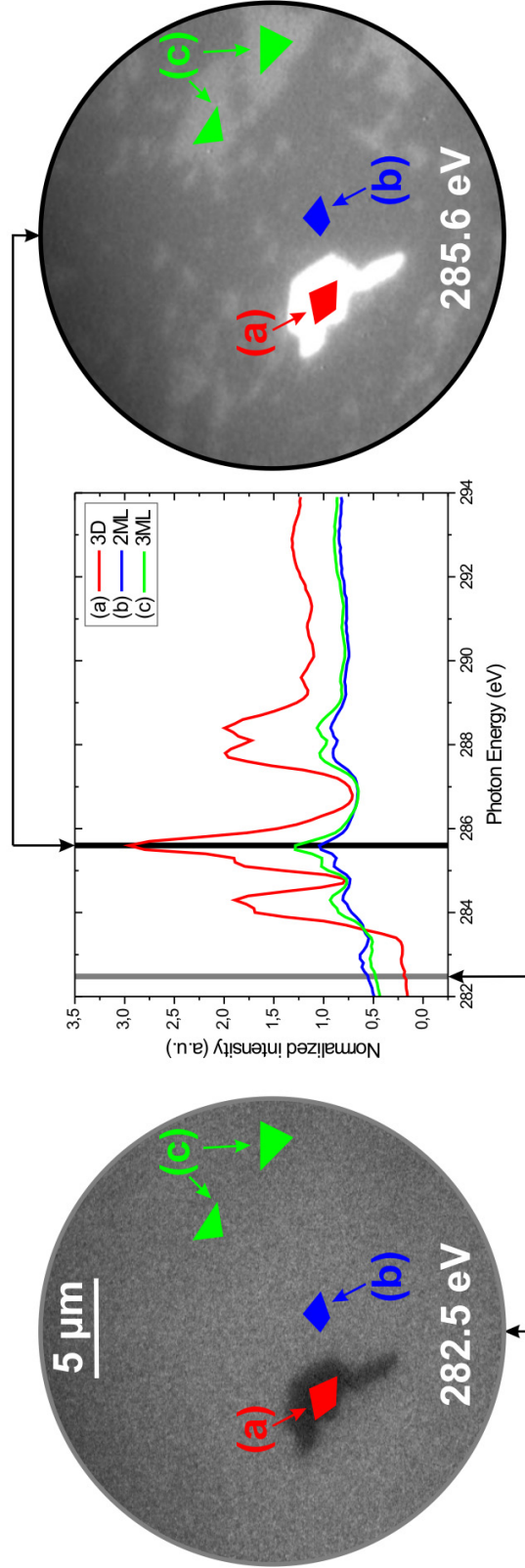
Figure 5.6: Laterally resolved NEXAFS: both XPEEM images show a nominal 5 ML thick PTCDA film grown at T = 303 K on the Ag(1 1 1) surface. The left image is taken at a photon energy of $h\nu = 282.5$ eV, the right at $h\nu = 285.6$ eV. In both cases the electrical field vector of the light is almost parallel to the surface normal (inclined of 20°). The emitted secondary electrons have been used for imaging. Inside the images three regions are marked by labels and the corresponding spectra analyzed in these marked areas are shown in the center (legend: PTCDA nominal thickness). Both XPEEM images, are rescaled for contrast enhancement.

is constant.

2. The emission from the substrate is reduced by elastic and inelastic scattering (attenuation). This results in a thickness sensitivity.

3. In resonance (which depends on the photon energy and the polarization of the incoming light) the intensity will increase with the thickness of the resonating material. This results in a thickness sensitivity *only* after the onset of the resonance.

4. The emission from inside the PTCDA material (in the case of the resonance as for point 3) is also reduced by elastic and inelastic scattering of the emitted electrons (attenuation).

The interplay of the above mentioned contributions to the overall NEXAFS intensity can be summarized in the following equation:

$$I(E_{\mathrm{ph}}, \vec{e}, n) = I_{\mathrm{subst.}}(E_{\mathrm{ph}}) \cdot \mathrm{e}^{-\alpha d n} \cdot f(\Phi_n) + \sum_{m=1}^{n} I_{\mathrm{PTCDA}}(E_{\mathrm{ph}}, \vec{e}, m) \cdot \mathrm{e}^{-\alpha d(n-m)} \cdot f(\Phi_n) \quad (5.3)$$

where E_{ph} is the photon energy, $\vec{e}$ is the x-ray light polarization vector[4], n is the total number of layers, α is damping constant, d is the interlayer distance, $f(\Phi_n)$ is the cut-off function and Φ_n is the work function.

The two terms of equation (5.3) describe the intensity originating from the substrate and the organic layer, respectively. The influence of the damping is described by the exponential terms. Before the onset of the resonance the second term of equation 5.3 is zero. It is therefore possible to calculate the IMFP from the ratio of the intensity for a fixed photon energy and of the 3-layer thick and 2-layer thick regions:

$$\frac{I(n=2)}{I(n=3)} = \frac{I_{\mathrm{subst.}} \cdot \mathrm{e}^{-2\alpha d} \cdot f(\Phi_2)}{I_{\mathrm{subst.}} \cdot \mathrm{e}^{-3\alpha d} \cdot f(\Phi_3)} = e^{\alpha d}$$

Using this calculation, the intensity attenuation of the 2nd and 3rd layer before the onset of the resonances (Fig. 5.6) yields an IMFP value of $\lambda = 1.9 \pm 0.3$ nm.

This value is almost twice the one obtained using a Hg-short arc lamp. This increase might be explained by the larger kinetic energy range of the secondary electrons

---

[4]The orientation of the molecules is fixed: parallel to the substrate.

detected by the NEXAFS method (about 5 to 7 eV wide, with an intensity maximum at approx. 3 eV) as compared to the quite narrow energy range of approx. 0.1–0.5 eV of Hg-PEEM. The IMFP value obviously varies in these different energy ranges (see also the red and blue markings in Fig. 5.5). An increase of the IMFP value from approx. 0.8 nm at 0.5 eV to more than 1.9 nm at 3 eV could explain the two different experimental results.

5.3 Image contrast in LEEM of organic layers on metals

As LEEM is the imaging counterpart of LEED, the most obvious contrast mechanism is based on local differences in the diffraction conditions, the so-called *diffraction contrast*. There are two modes of operation to exploit this contrast: the bright field and the dark field imaging mode. In the first case the specularly reflected beam — the so-called (00) beam — is used and is mainly sensitive to step contrast, reflectivity, and facets. The second mode selects a non-specularly diffracted beam for the imaging (different from the (00) beam), and it is mainly used to image superstructure domains. In bright field mode, the reflectivity contrast in the image will be obtained at the energy V_0 at which $I_{00}(V_0)$ varies between different regions. The $I_{00}(V_0)$ corresponds to the I(V) curve of the specularly reflected beam as often referred to by LEED users. These differences are caused by, e.g., changes in the crystal orientation and the structure, surface reconstruction or adsorbate islands vs. clean surface. Subsection 5.3.1 discusses contrast effects due to the presence of 3d-islands on the surface and the coexistence of rotational domains of organic thin films on metals.

A second wave-optical contrast mechanism is known as *interference contrast*. This does not involve directly the lateral periodicity of the substrate even though periodicity is (often) necessary to have sufficient LEEM intensity. There are two types of interference contrast and both arise from the interference of waves reflecting at different vertical heights in the sample: (a) the geometric phase contrast due to a wave reflecting from the upper and lower side of a step, and (b) the so-called quantum size contrast arising from the interference of a wave reflecting from the thin film surface

and the interface between this film and the substrate. The latter is a common phenomenon in the growth of thin films and can be quantitatively compared to the optical interference in thin films. Both, geometric phase and quantum interference are strictly related to the ratio λ/d, where λ is the electron wave length and d is either the step height or the film thickness. In subsection 5.3.2 the interference effects in organic thin films on metals are discussed.

5.3.1   Diffraction contrast in LEEM

In this subsection it will be described how the 3d-islands appear in the LEEM images and how the thin film geometrical orientation is visualized.

PTCDA forms crystallites on both, the Ag(1 1 1) and Au(1 1 1) surface, at temperatures above room temperature and up to 450 K, as will be shown in chapter 7. These 3D-islands have the (1 0 2) facets parallel to the substrate, and other facets form an angle of $\sim 21°$ with the substrate [34]. Figure 5.7 shows an example of how the 3D-islands appear with LEEM on a Au(1 1 1) surface (the same contrast conditions would be obtained on the Ag(1 1 1) surface). Notice that in figure 5.7 the side facets of the islands appear dark. At this kinetic energy, 2.2 eV, the imaging is said to be not in the *Bragg* condition and therefore the facet intensity was cut away by the contrast aperture. The kinetic energy dependence of the top facet of the crystallites and of the thin layers is discussed in subsection 5.3.2.

The growth of a thin film may occur with the formation of different rotational domains. For the case of the first two layers of PTCDA/Ag(1 1 1), only one structure is observed, at temperatures between 320 and 450 K [34]. This structure has three symmetry equivalent rotational times two reflection domains. A detailed analysis of the surface structure has been done using SPA-LEED (Spot-Profile-Analysis LEED) and is thoroughly described in the work of Kilian [38, 34]. In the following we combine μ-spot LEED and dark field imaging to observe the rotational domains on the surface and relate them to the morphology of the underlying substrate. These findings will be useful for the discussions in the following chapter where the relation between the substrate morphology and the growth properties is investigated.

Figure 5.8.a shows a LEEM image at 2 eV with a 20 μm aperture placed around
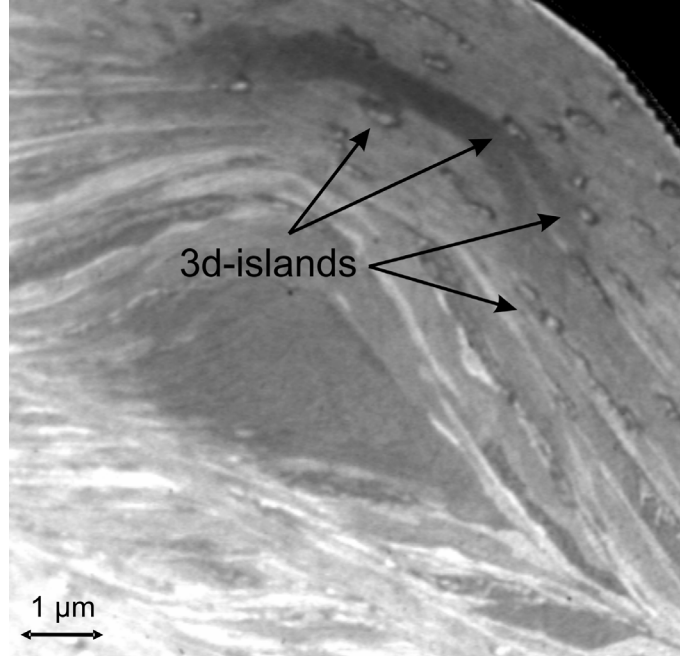
Figure 5.7: LEEM of 5 ML of PTCDA on Au(1 1 1) at 2.2 eV and 353 K. The facets of the 3D-islands, some of which are marked by arrows, appear dark.

the (00) spot of the reflected beam. The bright regions in the image are those covered by one layer of PTCDA, while the darker regions are those due to the bare Ag(1 1 1) surface. Within the one layer thick PTCDA covered regions the small dark lines are single steps, while the thicker lines are attributed to step bunches. The fact that the whole PTCDA covered region has the same intensity, i.e. $I_{00}(V_0 = 2\,\mathrm{eV}) = \mathrm{const.}$, can be related to a constant *vertical* height, but not directly to a constant *horizontal* periodicity. The latter is addressed by dark field imaging. The yellow circle identifies a region of 180 $\mu\mathrm{m}^2$ used for the LEED image shown in figure 5.8.b. The LEED pattern stems mainly from two orientational domains. The complete LEED pattern in figure 5.8.c was obtained by averaging over many orientational domains[5]. The double-triangle structure inside the ellipse originates from all possible PTCDA domains on the surface (six in total). We have tilted the incoming beam (to the surface) so that the three regions marked in figure 5.8.b would pass through the contrast aperture.

---

[5]The position of the diffraction spots with conventional LEED methods depends on the energy, while in a microscope it depends on the imaging settings.
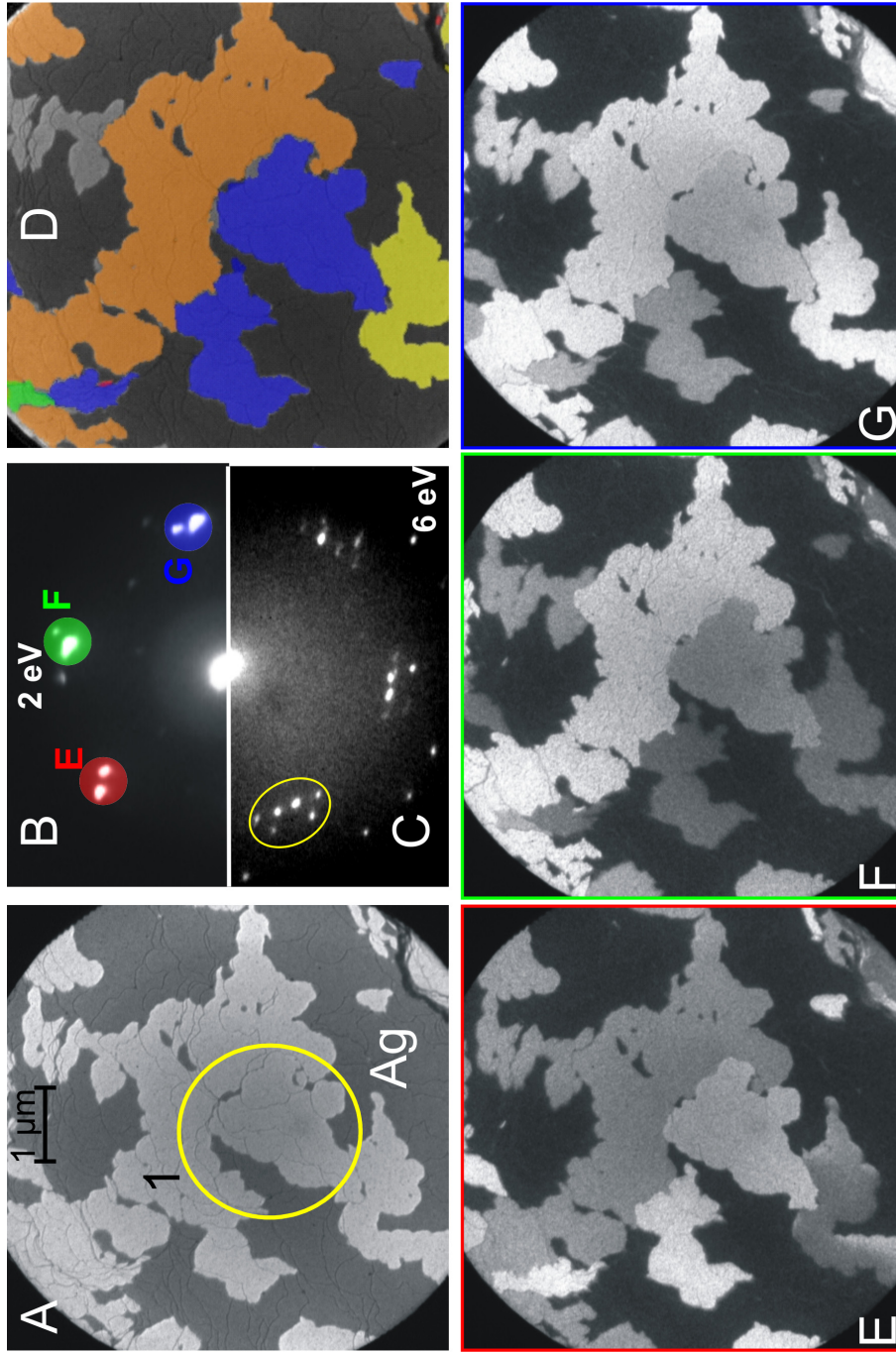
Figure 5.8: Rotational domains in LEEM: 0.5 ML of PTCDA on Ag(111). All images have been taken at 2 eV of kinetic energy. (a) LEEM image, 6 μm field of view. (b) μ-spot LEED taken from the area marked by a yellow circle in image (a). (c) LEED image averaging over many domains. (d) identification of orientational domains as obtained from the dark field imaging using the diffraction spots labelled (E), (F) and (G) in the LEED image (b). The dark field images are displaced in frames (e), (f) and (g).

The diffraction spots from all possible domains are not separated enough to have the dark-field image originating from only one rotational domain. This results in different intensities for the different domains as shown in figure 5.8.e–g, while for *ideal* dark field imaging only *one* single domain should be bright and the rest dark.

Interestingly, not every substrate single step acts as a boundary for the orientational domains. This indicates that the growth can proceed across single steps and that the long-range lateral order, due to the in-plane interaction, can be sustained across single steps. In contrast, domain boundaries are also often located at step bunches. These are considerations that are useful for the discussions in the following chapter.

5.3.2   Interference contrast in LEEM

As already mentioned, an electron wave reflecting from the higher and lower side of a step or from the surface of a thin film and from the interface of the thin film to the substrate, interferes, and important information may be extracted from the resulting intensity modulation. As an example, the asymmetry in the contrast at steps can be used to determine on which side of the step is the higher or lower terrace [63]. In our work, the interference at steps is very useful for the identification of single and multiple steps. The single step resolution is achieved by slight defocusing of the objective lens, and the step contrast results from the phase difference between the wave reflected at the top and bottom side of the step. As shown by *Tromp et al.* [64], LEEM is suited for the investigation of buried interfaces. The single steps on the substrate, buried under the PTCDA monolayer, can be imaged as shown in figure 5.8.a. The combination of LEEM imaging, for identification of steps and step bunches *and* rotational domains (discussed in the last section), with UV-PEEM during the growth of PTCDA thin films on Ag(1 1 1) has led to a detailed understanding of the kinetic processes. The results are presented in chapter 6 on page 61.

We have measured the intensity of the elastically reflected electrons as a function of the kinetic energy. We observed intensity oscillations in the low kinetic energy regime (< 10 eV) which are associated with quantum well resonances above the vacuum level. The results for a 5 ML thick film on the Au(1 1 1) surface are shown in figure 5.9. The kinetic energy scale of the plot is referenced to the vacuum level as determined
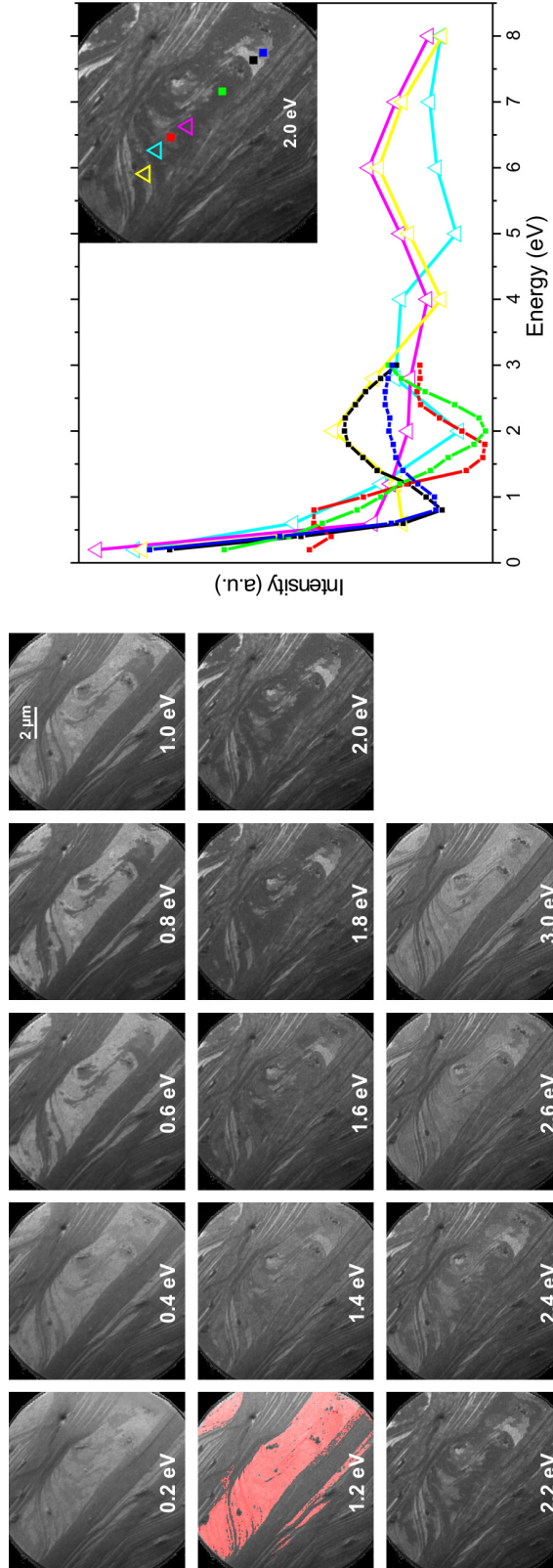
Figure 5.9: Quantum size interference in LEEM for five nominal layers of PTCDA/Au(1 1 1) at 380 K. The Au(1 1 1) surface is composed of regions with terraces, crossed mainly by single steps (red region in the image at 1.2 eV), and large regions with step bunches. Left: set of images at different electron kinetic energies. Right: plot of the LEEM intensity $I_{00}(E)$ for the regions marked in the inset.

by measuring the onset of perfect reflection from the surface. This accounts for a difference in the work functions of the surface and the cathode. In the graph the oscillatory behavior of the intensity is plotted for different surface regions as marked in the image in the inset. Two prominent maxima are found in the spectra at approx. 2 eV and 6 eV and two minima at approx. 2 eV and 1.8 eV[6]. The differences between the curves arise from different film thicknesses. Apart from the obvious enhancement of the contrast, the interference peaks observed can be analyzed for a deeper investigation of the quantum well resonances. These resonances obviously depend on two experimental parameters, the kinetic energy and the thickness, but also on other intrinsic solid state properties of the thin film. For example, in a nearly free electron model description three free parameters have to be determined such as the mean crystal potential V_0 (offset of the periodic potential), the pseudopotential form factor U (amplitude of the periodic potential) and the electron effective mass m^*. We unfortunately do not have the statistics to determine the three parameters because the interference peaks observed are too few and cannot be correlated to the thickness. Any attempt to apply a simpler description, i.e. a free electron model, would not account for the linear dependence between the kinetic energy and the phase shift [65].

However, this is the first experimental observation of a quantum size effect in the propagation of an electron wave in an organic thin film with LEEM. The systematic investigation of these systems with careful control of the beam damage [26] and the film thickness can add insight into the properties of the buried interface (such as strees or the reflection phase [66]).

---

[6]We have measured up to kinetic energies of 8 eV. Higher energies would cause a considerable damage to the thin film. The peaks below approx. 1 eV are not considered because they overlap with the onset of mirror reflection.